

Three-Dimensional Cole-Cole Model Inversion of Induced Polarization Data Based on Regularized Conjugate Gradient Method

Zhengwei Xu and Michael S. Zhdanov

Abstract—Modeling of induced polarization (IP) phenomena is important for developing effective methods for remote sensing of subsurface geology. However, the quantitative interpretation of IP data in a complex 3-D environment is still a challenging problem of applied geophysics. This letter develops a method of determining a 3-D distribution of the four parameters of the Cole-Cole model based on surface IP data. The method takes into account the nonlinear nature of both electromagnetic induction and IP phenomena. The solution of the 3-D IP inverse problem is based on the regularized conjugate gradient method. The method was tested on a synthetic model with variable dc conductivity, intrinsic chargeability, time constant, and relaxation parameters, and it was also applied to the actual 3-D IP survey data. We demonstrate that the four parameters of the Cole-Cole model, namely, dc electrical resistivity, chargeability, time constant, and the relaxation parameter, can be recovered from the observed IP data simultaneously.

Index Terms—Cole-Cole model, induced polarization (IP), inversion, regularized conjugate gradient method (RCGM).

I. INTRODUCTION

THIS letter focuses on using a land-based controlled source electromagnetic (EM) method for detecting geoelectrical anomalies in the subsurface. The EM data observed in a geophysical survey generally reflect two phenomena: 1) EM induction (EMI) in the earth and 2) induced polarization (IP) effects related to the relaxation of polarized charges in rock formations. The EMI effect can be simulated by the solution of the Maxwell's equations in the geoelectrical model characterized by frequency-independent conductivity. Polarization is usually based on models with a frequency-dependent conductivity distribution. One of the most popular models is the Cole-Cole relaxation model [1]. This model was introduced for studying the IP effect in the pioneering papers of Pelton [2], [3].

Manuscript received September 7, 2014; revised November 9, 2014; accepted December 1, 2014. This work was supported in part by the University of Utah Consortium for Electromagnetic Modeling and Inversion, TechnoImaging, and Moscow Institute of Physics and Technology.

Z. Xu is with the Consortium for Electromagnetic Modeling and Inversion, University of Utah, Salt Lake City, UT 84112 USA (e-mail: zhengweixu.usa@gmail.com).

M. S. Zhdanov is with the Consortium for Electromagnetic Modeling and Inversion, University of Utah, Salt Lake City, UT 84112 USA, with TechnoImaging, Salt Lake City, UT 84107 USA, and also with the Moscow Institute of Physics and Technology, Moscow 141700, Russia (e-mail: michael.s.zhdanov@gmail.com).

Color versions of one or more of the figures in this paper are available online at <http://ieeexplore.ieee.org>.

Digital Object Identifier 10.1109/LGRS.2014.2387197

The Cole-Cole model has been used in a number of publications for the interpretation of IP data [4]–[8]. The parameters of the conductivity relaxation model can be used for the discrimination of different types of rock formations, which is an important goal in mineral and petroleum exploration [9], [10]. It was demonstrated by Zhdanov [11] that the Cole-Cole model can be derived analytically from the general formulas of the generalized effective-medium theory of IP (GEMTIP) in the case of a conductive media with spherical polarized inclusions.

The quantitative interpretation of IP data in a complex 3-D environment is a very challenging problem because of the coupling between the IP and EMI effects. Many published algorithms are based on a linear or a quasi-linear approximation of the IP response. However, the Cole-Cole parameters can be recovered more accurately by using a nonlinear inversion based on rigorous forward modeling. This letter develops a technique for 3-D nonlinear inversion of IP data based on the Cole-Cole relaxation model and for a multitransmitter configuration typical in IP surveys in the field.

II. FORWARD MODELING OF IP BASED ON THE INTEGRAL EQUATION METHOD

Let us consider a 3-D geoelectrical model with a horizontally layered background conductivity σ_b and a local inhomogeneous region D , with an arbitrarily varying complex conductivity $\sigma = \sigma_b + \Delta\sigma$. Based on the integral equation method [12], it is possible to determine the EM field of an arbitrary current distribution j within a medium with background conductivity σ_b using the following equations:

$$\mathbf{E}(\mathbf{r}_j) = \iiint_D \widehat{\mathbf{G}}_{\mathbf{E}}(\mathbf{r}_j|\mathbf{r}) \cdot \mathbf{j}(\mathbf{r}) dv = \mathbf{G}_{\mathbf{E}}(\mathbf{j}) \quad (1)$$

$$\mathbf{H}(\mathbf{r}_j) = \iiint_D \widehat{\mathbf{G}}_{\mathbf{H}}(\mathbf{r}_j|\mathbf{r}) \cdot \mathbf{j}(\mathbf{r}) dv = \mathbf{G}_{\mathbf{H}}(\mathbf{j}) \quad (2)$$

where $\widehat{\mathbf{G}}_{\mathbf{E}}(\mathbf{r}_j|\mathbf{r})$ and $\widehat{\mathbf{G}}_{\mathbf{H}}(\mathbf{r}_j|\mathbf{r})$ are the electric and magnetic Green's tensors defined for an unbounded conductive medium with the background (horizontally layered) conductivity σ_b , respectively; $\mathbf{G}_{\mathbf{E}}$ and $\mathbf{G}_{\mathbf{H}}$ are the electric and magnetic Green's operators, respectively.

The anomalous fields generated by the excess current \mathbf{j}^a induced within the domain with anomalous conductivity $\Delta\sigma$ can be expressed as follows:

$$\mathbf{E}^a(\mathbf{r}_j) = \iiint_D \widehat{\mathbf{G}}_{\mathbf{E}}(\mathbf{r}_j|\mathbf{r}) \cdot \mathbf{j}^a(\mathbf{r}) dv = \iiint_D \widehat{\mathbf{G}}_{\mathbf{E}}(\mathbf{r}_j|\mathbf{r}) \cdot \Delta\sigma(\mathbf{r})\mathbf{E}(\mathbf{r}) dv = \mathbf{G}_{\mathbf{E}}(\mathbf{j}^a) \quad (3)$$

$$\mathbf{H}^a(\mathbf{r}_j) = \iiint_D \widehat{\mathbf{G}}_{\mathbf{H}}(\mathbf{r}_j|\mathbf{r}) \cdot \mathbf{j}^a(\mathbf{r}) dv = \iiint_D \widehat{\mathbf{G}}_{\mathbf{E}}(\mathbf{r}_j|\mathbf{r}) \cdot \Delta\sigma(\mathbf{r}) \mathbf{E}(\mathbf{r}) dv = \mathbf{G}_{\mathbf{H}}(\mathbf{j}^a) \quad (4)$$

where $\mathbf{j}^a = \Delta\sigma$.

Using integral (3) and (4), one can calculate the EM field at any point \mathbf{r}_j if the electric field is known within inhomogeneity, D .

It was demonstrated in the pioneering work of Pelton [2] that the Cole-Cole relaxation model can represent well the typical complex resistivity of a polarized rock formation. In the framework of this model, the complex resistivity $\rho(\omega)$ is described by the following expression:

$$\rho\omega = \rho_0 \left(1 - \eta \left(1 - \frac{1}{1 + (i\omega\tau)C} \right) \right) \quad (5)$$

where σ_0 is the dc resistivity (in $\Omega \cdot \text{m}$), ω is the angular frequency (in rad/s), τ is the time parameter, η is the intrinsic chargeability [14], and C is the relaxation parameter. The dimensionless intrinsic chargeability η characterizes the intensity of the IP effect. These four parameters represent the properties of the rocks that may allow the researcher to distinguish between the different types of rocks [9], [10].

A typical IP survey consists of multiple electric dipole transmitters and receivers. The integral equation method can be used for 3-D modeling of both EMI and IP effects in inhomogeneous structures. In this case, (3) and (4) should be modified to take into account the IP effect. The main modification includes an expression for the anomalous conductivity $\Delta\sigma$, which should be substituted now by another complex value $\Delta\tilde{\sigma}(\omega)$ [12]. In order to take into account the IP effect, one should assume that the conductivity within the anomalous domain $\sigma_b + \Delta\tilde{\sigma}$ becomes complex and frequency-dependent, i.e.,

$$\sigma_b + \Delta\tilde{\sigma} = \sigma(\omega) = 1/\rho(\omega). \quad (6)$$

We also consider that the complex resistivity $\rho(\omega)$ is described by the relaxation Cole-Cole model [see (5)]. Thus, the anomalous conductivity $\Delta\tilde{\sigma}$ can be expressed as follows:

$$\Delta\tilde{\sigma} = \sigma(\omega) - \sigma_b \quad (7)$$

where

$$\sigma(\omega) = \sigma_0 \left(1 - \eta \left(1 - \frac{1}{1 + (i\omega\tau)C} \right) \right)^{-1} \quad (8)$$

and $\sigma_0 = 1/\rho_0$.

Equation (7) can be rewritten in the following compact form:

$$\Delta\tilde{\sigma} = \sigma f(\eta, \tau, C) - \sigma_b \quad (9)$$

where function $f(\eta, \tau, C)$ is represented by the following expression:

$$f(\eta, \tau, C) = \left(1 - \eta \left(1 - \frac{1}{1 + (i\omega\tau)C} \right) \right)^{-1}. \quad (10)$$

According to (3) and (4), the anomalous EM field is related to the electric current induced in the inhomogeneity, i.e., $\mathbf{j}^a = \Delta\tilde{\sigma} \mathbf{E}$, by the following integral formulas:

$$\mathbf{E}^a(\mathbf{r}_j) = \iiint_D \widehat{\mathbf{G}}_{\mathbf{E}}(\mathbf{r}_j|\mathbf{r}) \cdot \Delta\tilde{\sigma} \mathbf{E} dv = A_{\mathbf{E}}(\Delta\tilde{\sigma}) \quad (11)$$

$$\mathbf{H}^a(\mathbf{r}_j) = \iiint_D \widehat{\mathbf{G}}_{\mathbf{H}}(\mathbf{r}_j|\mathbf{r}) \cdot \Delta\tilde{\sigma} \mathbf{E} dv = A_{\mathbf{H}}(\Delta\tilde{\sigma}) \quad (12)$$

where $A_{\mathbf{E}}$ and $A_{\mathbf{H}}$ are electric and magnetic integral operators, respectively, and domain D represents a volume with the anomalous conductivity distribution $\sigma(r) = \sigma_b(r) + \Delta\tilde{\sigma}(r)$, $D \ni r$.

In numerical notation, we can describe the forward modeling problem (11) and (12) as a matrix operator equation, i.e.,

$$\hat{d} = \hat{A}(\hat{m}) \quad (13)$$

where \hat{d} is a column matrix representing the electric or magnetic data in a discrete number of observation points and for a specific set of frequencies; \hat{m} is a column matrix representing the distribution of the model parameters (anomalous conductivities $\Delta\tilde{\sigma}$) in the nodes of a discrete grid covering domain D ; and matrix operator $\hat{A}(\hat{m})$ represents in a discrete form the integral operators $A_{\mathbf{E}}$ or $A_{\mathbf{H}}$ for electric or magnetic fields, respectively.

III. INVERSION METHODOLOGY

The inverse problem (13) is ill-posed, i.e., the solution can be nonunique and unstable. The traditional way to obtain the regularized solution of this equation is based on introducing the Tikhonov parametric functional, i.e.,

$$P^\alpha(\hat{m}) = \varphi_w(\hat{m}) + \alpha s_w. \quad (14)$$

In the last formula, $\varphi_w(\hat{m})$ is the data-weighted misfit functional between the predicted data $\hat{A}(\hat{m})$ and the observed data \hat{d} , i.e.,

$$\varphi_w(\hat{m}) = \left(\widehat{W}_d \hat{A}(\hat{m}) - \widehat{W}_d \hat{d} \right)^* \left(\widehat{W}_d \hat{A}(\hat{m}) - \widehat{W}_d \hat{d} \right) \quad (15)$$

and $s_w(\hat{m})$ is the model-weighted stabilizing functional that is usually introduced as the least squares difference between the regularized solution and some *a priori* model \hat{m}_{apr} , i.e.,

$$s_w(\hat{m}) = \left(\widehat{W}_m \hat{m} - \widehat{W}_m \hat{m}_{\text{apr}} \right)^* \left(\widehat{W}_m \hat{m} - \widehat{W}_m \hat{m}_{\text{apr}} \right) \quad (16)$$

where \widehat{W}_d and \widehat{W}_m are the data and model weighting matrices, respectively [15], and the asterisk * denotes a complex conjugate transposed matrix.

The data weighting matrix \widehat{W}_d is selected as a diagonal matrix of the inverse magnitudes of the background electric field, i.e.,

$$\widehat{W}_d = \text{diag} \left[|E^b|^{-1} \right]. \quad (17)$$

The model weighting matrix is determined according to the following formula:

$$\widehat{W}_m = \sqrt[4]{\hat{F}_m^T \cdot \hat{F}_m} \quad (18)$$

where \hat{F}_m is the Fréchet derivative of the forward operator \hat{A} . This choice of model weighting matrix ensures a uniform sensitivity to the different model parameters [15]. Appendix shows that the linear Fréchet derivative operator can be represented as a product of the matrix of the Fréchet derivative of the original forward modeling operator and the partial derivatives of the anomalous conductivity with respect to the four Cole-Cole model parameters σ , η , τ , and C .

According to the basic principles of the regularization method, we have to find a model \hat{m}_a , a quasi-solution of the inverse problem, that minimizes the parametric functional

$$P^\alpha(\hat{m}, \hat{d}) = \min. \quad (19)$$

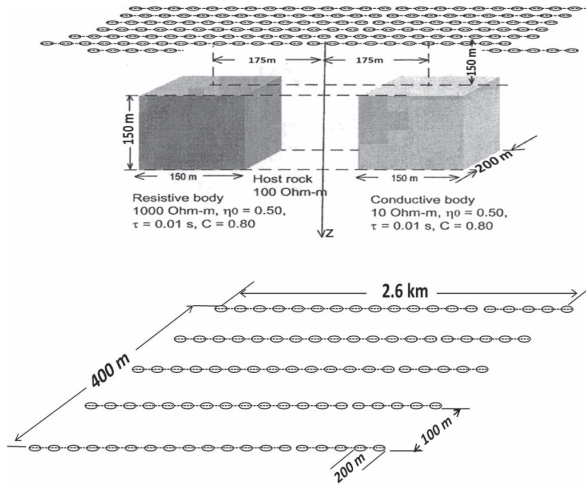


Fig. 1. (a) Two rectangular conductive and resistive bodies in a $100\text{-}\Omega \cdot \text{m}$ homogenous background. (b) Configuration of the IP survey.

TABLE I
COLE-COLE PARAMETERS OF CONDUCTIVE AND RESISTIVE BODIES

| | Conductive body | Resistive body |
|-------------------------|--------------------|------------------------|
| ρ_0 (σ_0) | 10 Ohm-m (0.1 S/m) | 1000 Ohm-m (0.001 S/m) |
| η | 0.5 | 0.5 |
| τ | 0.01 | 0.01 |
| C | 0.8 | 0.8 |

Note that the solution of this problem is equivalent to the minimization of the stabilizing functional

$$s_w(\hat{m}) = \left(\widehat{W}_m \hat{m} - \widehat{W}_m \hat{m}_{\text{apr}} \right)^* \left(\widehat{W}_m \hat{m} - \widehat{W}_m \hat{m}_{\text{apr}} \right) = \min \quad (20)$$

under the condition that the misfit is equal to the given level of the noise in the data

$$\varphi_w(\hat{m}) = \left(\widehat{W}_d \hat{A}(\hat{m}) - \widehat{W}_d \hat{d} \right)^* \left(\widehat{W}_d \hat{A}(\hat{m}) - \widehat{W}_d \hat{d} \right) = \delta. \quad (21)$$

We apply the regularized conjugate gradient method (RCGM) to the solution of this problem. The iterative process of RCGM is terminated based on the conventional misfit condition of the regularization theory when the misfit reaches the noise level [15].

IV. MODEL STUDY

In our model study, we used the geoelectrical model similar to one introduced in [6], which consists of two rectangular conductive and resistive bodies submerged in a $100\text{-}\Omega \cdot \text{m}$ homogenous background [see Fig. 1(a)]. The tops of the bodies are located at a depth of 100 m. The body sides in the x , y , and z directions have a length of 150, 200, and 150 m, respectively. The IP parameters of the conductivity defined by the Cole-Cole model (8) are shown in Table I. These four IP parameters were assumed to be unknown, and the inversion was run for these four parameters simultaneously.

The EM field in this model is generated by electric bipole transmitters with a length of $a = 100$ m (galvanic EM field excitation) and is measured by electric bipole receivers of the same length. The transmitters and receivers are positioned along a system of profiles shown in Fig. 1(b). For each transmitter position, there are up to six receivers located at distances na

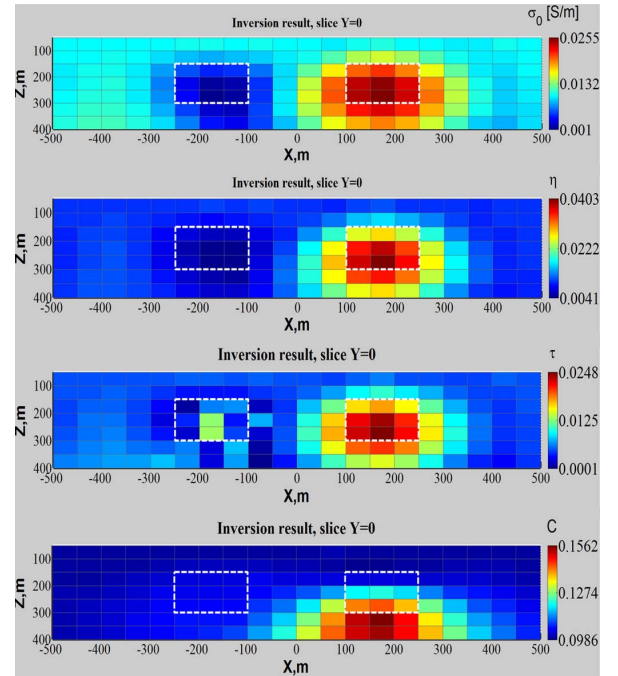


Fig. 2. Vertical sections ($y = 0$ m) of 3-D synthetic inversion results with respect to each of the Cole-Cole model parameters σ , η , τ , and C , from the top to bottom.

from the end of the bipole transmitter, where $n = 1, 2, \dots, 6$, respectively. Thus, there are 25 transmitters in one profile of 2.6 km in length [see Fig. 1(b)]. For the transmitters located at the right-hand side of the profile, the number of the corresponding receivers is reduced respectively so that, for transmitter number 25, there is just one receiver.

The synthetic EM data for this model were generated using the integral equation forward modeling code. We used eight frequencies: 0.25, 0.5, 1, 2, 4, 8, 16, and 32 Hz. The area of the inversion was subdivided into 1960 cells ($20 \times 14 \times 7$), with the size of each cubic cell being $50 \text{ m} \times 50 \text{ m} \times 50 \text{ m}$. The inversion was run simultaneously for the four parameters, namely, σ_0 , η , τ , and C . The computations were run on a single Linux Workstation with eight processors (2.5 GHz) and 32-GB memory using the MATLAB parallel computation function. It took about 8 h for inversion to reach a misfit at a noise level of 8% after about 100 iterations.

Fig. 2 shows the inversion results represented as x - z sections ($y = 0$ m) of the dc conductivity σ_0 , chargeability η , time parameter τ , and relaxation parameters C . One can see that, for a conductive body, the inversion results look very good for the conductivity σ_0 , chargeability η , and time parameter τ . For relaxation parameter C , the position of the anomaly is lower than that of its true position, which reflects the known fact that the IP data have relatively low sensitivity to C . The Cole-Cole parameters of the resistive body are not recovered well due to the low sensitivity of the IP response to the resistive body.

V. CASE STUDY: IP SURVEY IN THE AREA OF NORTH SILVER BELL DEPOSIT

The Silver Bell district is located within the porphyry copper province of southwestern North America, approximately 35 mi northwest of Tucson, AZ, on the south side of the Silver Bell

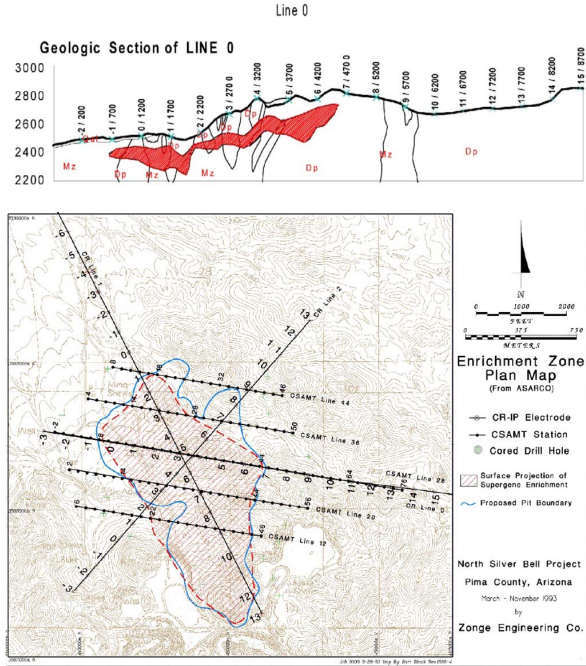


Fig. 3. (Top) Geological section along IP survey Line 0. (Bottom) Map of the enrichment zone and the IP survey lines (after [17]).

Mountains. Mineralization in the district consists of at least three distinct disseminated porphyry copper deposits and several skarn replacement deposits. Disseminated primary and supergene enriched porphyry copper mineralization were mined in two open pits, namely, E1 Tiro and Oxide, by ASARCO, mainly between 1954 and 1977. The total production for that period was reported at 75.66 million tons (Mt) at 0.80% copper [16]. The North Silver Bell deposit is located at the north end of the district and represents a leachable resource of in excess of 80 Mt at an average grade of 0.40% copper contained mostly within an enrichment blanket of chalcocite.

A reconnaissance IP survey was conducted in the North Silver Bell area by Zonge Engineering to assess the utility of this technique in defining a porphyry system [17]. One IP survey Line 0 shown in Fig. 3 (bottom) was surveyed at North Silver Bell using a dipole spacing of 500 ft. It served as the central line for the CSAMT and magnetic surveys. The orientation of the line was chosen to minimize the extremes of the crossed topography and to be perpendicular to an inferred major fault. The data for Line 0 were acquired with a Zonge GDP-16 three-channel receiver in a reference complex-resistivity mode using 15 harmonic frequencies from 0.125 to 72 Hz generated by the three main frequencies of the current in the transmitters.

The apparent resistivity and IP phase were converted into the real and imaginary parts of the electric field, which served as the input data for the inversion. The IP data were inverted for a 3-D conductivity model with 4669 cells of size $100 \text{ m} \times 300 \text{ m} \times 50 \text{ m}$. The inversion domain was selected from -100 to 2800 m along the survey line, from -1050 to 1050 m across the survey line and from 50 to 1200 m in the vertical direction. The initial and *a priori* models for 3-D inversion with respect to each of the parameters σ_0 , η , τ , and C were selected as follows:

$$\begin{aligned} \sigma_{\text{init}} &= \sigma_{\text{apr}} = \frac{1}{500} \text{ S/m}; & \eta_{\text{init}} &= 0.01, \eta_{\text{apr}} = 0 \\ \tau_{\text{init}} &= 0.01, \tau_{\text{apr}} = 0; & C_{\text{init}} &= 0.01, C_{\text{apr}} = 0. \end{aligned}$$

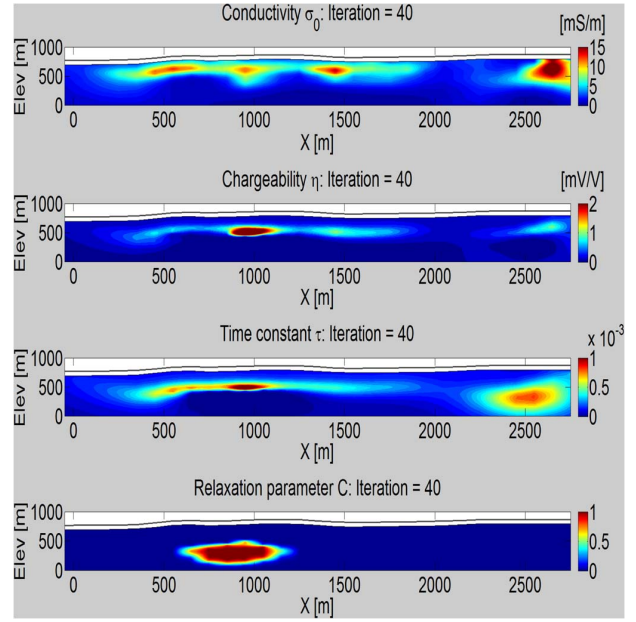


Fig. 4. Vertical sections of 3-D inversion results beneath the IP survey Line 0 with respect to each of the Cole-Cole model parameters σ_0 , η , τ , and C .

The 3-D inversion for the IP data converged to a final misfit of 10% (a noise level in the observed data) after about 40 h. Fig. 4 shows a vertical cross section of the 3-D model beneath the survey line with respect to each of the parameters σ_0 , η , τ , and C . The IP inversion results correlate well with the known geological section of the IP survey, as shown in Fig. 3 (top). From the inversion results for σ_0 , η , τ , and C , one can see that the corresponding lateral conductive body corresponds well to the phyllic alteration zone within which abundant pyrite and chalcopyrite are contained. However, in the inversion result for C , it seems that the anomalous body of C is much deeper than those of other three parameters, but it is still in the area of the target. Note that we observed a similar result for the synthetic model. The main reason is that the sensitivity of the IP data with respect to the relaxation parameter C is the weakest among the four Cole-Cole model parameters.

VI. CONCLUSION

This letter develops a method of 3-D simultaneous inversion of the four parameters of the Cole-Cole model, namely, σ_0 , η , τ , and C , from the surface IP data. The new method considers both EMI and IP effects and determines the Cole-Cole model parameters using the RCGM. The advantage of our method over the published algorithms is that we take into account the nonlinear effects in the IP data by computing the forward modeling response rigorously using the 3-D integral equation forward modeling method.

With a synthetic model, we have shown the ability of the inversion method to accurately recover the 3-D distribution of the four Cole-Cole parameters for a conductive body. The method was also applied to the field IP survey data from the North Silver Bell, located 35 mi northwest of Tucson, AZ, on the south side of the Silver Bell Mountains. The inversion results provided geoelectrical models that agreed well with the known geology of the area. Thus, we have demonstrated

that the four parameters of the Cole-Cole model, namely, dc electrical conductivity σ_0 , chargeability η , time constant τ , and relaxation parameter C , can be recovered from the observed IP data simultaneously.

We should note that the Cole-Cole model can be treated as a special case for spherical inclusions of a more general GEMTIP model of the polarizable medium, as introduced in [11]. Our method can be extended to the case of GEMTIP model parameters inversion, which will be a subject of future publications.

APPENDIX FRÉCHET DERIVATIVE CALCULATION FOR THE COLE-COLE MODEL PARAMETERS

The matrix of the Fréchet derivative \hat{F}_m is formed by a product of the matrix of the Fréchet derivative of the original forward modeling operator and partial derivatives of the anomalous conductivity with respect to the four Cole-Cole model parameters. Indeed, by applying the variation operator δ to the operator of forward modeling of the electric field A_E and using the chain rule of differentiation, we obtain the following equation:

$$\begin{aligned} \delta A_E &= F_E \delta_\sigma \Delta \tilde{\sigma} + F_E \delta_\eta \Delta \tilde{\sigma} + F_E \delta_\tau \Delta \tilde{\sigma} + F_E \delta_C \Delta \tilde{\sigma} \\ &= \left[F_E f(\eta, \tau, C), F_E \sigma \frac{\partial f(\eta, \tau, C)}{\partial \eta}, F_E \sigma \frac{\partial f(\eta, \tau, C)}{\partial \tau}, \right. \\ &\quad \left. F_E \sigma \frac{\partial f(\eta, \tau, C)}{\partial C} \right] \begin{bmatrix} \delta_\sigma \\ \delta_\eta \\ \delta_\tau \\ \delta_C \end{bmatrix} \end{aligned} \quad (1a)$$

where F_E is the Fréchet derivative matrix of the original forward modeling operator A_E , represented by the integral equation (11). This Fréchet derivative can be found using the corresponding perturbation of the anomalous field $E^a(r_j)$ [15]. From (1a), we derive that the Fréchet derivative matrix \hat{F}_m of nonlinear IP forward modeling operator A is given by the following expression:

$$\hat{F}_m = \left[F_E f(\eta, \tau, C), F_E \sigma \frac{\partial f(\eta, \tau, C)}{\partial \eta}, F_E \sigma \frac{\partial f(\eta, \tau, C)}{\partial \tau}, F_E \sigma \frac{\partial f(\eta, \tau, C)}{\partial C} \right] \quad (2a)$$

where

$$\begin{aligned} \frac{\partial f(\eta, \tau, C)}{\partial \eta} &= \frac{\partial}{\partial \eta} \left(1 - \eta \left(1 - \frac{1}{1 + (i\omega\tau)^C} \right) \right)^{-1} \\ &= \left(1 - \eta \left(1 - \frac{1}{1 + (i\omega\tau)^C} \right) \right)^{-2} \\ &\quad \times \left(1 - \frac{1}{1 + (i\omega\tau)^C} \right) \end{aligned} \quad (3a)$$

$$\begin{aligned} \frac{\partial f(\eta, \tau, C)}{\partial \tau} &= \frac{\partial}{\partial \tau} \left(1 - \eta \left(1 - \frac{1}{1 + (i\omega\tau)^C} \right) \right)^{-1} \\ &= -\eta (i\omega)^C \cdot \tau^{C-1} \cdot \left(1 - \eta \left(1 - \frac{1}{1 + (i\omega\tau)^C} \right) \right)^{-2} \\ &\quad \times (1 + (i\omega\tau)^C)^{-2} \end{aligned} \quad (4a)$$

$$\begin{aligned} \frac{\partial f(\eta, \tau, C)}{\partial C} &= \frac{\partial}{\partial C} \left(1 - \eta \left(1 - \frac{1}{1 + (i\omega\tau)^C} \right) \right)^{-1} \\ &\quad \cdot \left(1 - \eta \left(1 - \frac{1}{1 + (i\omega\tau)^C} \right) \right)^{-2} \\ &\quad \times (1 + (i\omega\tau)^C)^{-2}. \end{aligned} \quad (5a)$$

ACKNOWLEDGMENT

The authors would like to thank Zonge International and S. Urquhart for providing the IP data and for permission to publish the results.

REFERENCES

- [1] K. S. Cole and R. H. Cole, "Dispersion and absorption in dielectrics," *J. Chem. Phys.*, vol. 9, no. 4, pp. 343–351, Apr. 1941.
- [2] W. H. Pelton, "Interpretation of induced polarization and resistivity data," Ph.D. dissertation, Dept. Geol. Geophys., Univ. Utah, Salt Lake City, UT, USA, 1977.
- [3] W. H. Pelton, S. H. Ward, P. G. Hallof, W. R. Sill, and P. H. Nelson, "Mineral discrimination and removal of inductive coupling with multifrequency IP," *Geophysics*, vol. 43, no. 3, pp. 588–609, Apr. 1978.
- [4] P. Rowston, S. Busutil, and G. McNeill, "Cole-Cole inversion telluric cancelled IP data," *ASEG, Extended Abstracts*, vol. 2, pp. 1–4, 2003.
- [5] P. S. Routh and D. W. Oldenburg, "Electromagnetic coupling in frequency-domain induced polarization data: A method for removal," *Geophys. J. Int.*, vol. 145, no. 1, pp. 59–76, Apr. 2001.
- [6] K. Yoshioka and M. S. Zhdanov, "Three-dimensional nonlinear regularized inversion of the induced polarization data based on the Cole-Cole model," *Phys. Earth Planetary Interiors*, vol. 150, no. 1–3, pp. 29–43, May 2005.
- [7] D. Yuval and D. W. Oldenburg, "Computation of Cole-Cole parameters from IP data," *Geophysics*, vol. 62, no. 2, pp. 436–448, Mar. 1997.
- [8] W. Zhang, J.-X. Liu, Z.-W. Guo, and X.-Z. Tong, "Cole-Cole model based on the frequency-domain IP method of forward modeling," in *Proc. Progr. Electromagn. Res. Symp.*, 2010, Xi'an, China, pp. 383–386.
- [9] K. L. Zonge and J. C. Wynn, "Recent advances and applications in complex resistivity measurements," *Geophysics*, vol. 40, no. 5, pp. 851–864, Oct. 1975.
- [10] K. L. Zonge, "Method using induced polarization for ore discrimination in disseminated earth deposits," U.S. Patent 3 967 190, Jun. 29, 1976.
- [11] M. S. Zhdanov, "Generalized effective-medium theory of induced polarization," *Geophysics*, vol. 73, no. 5, pp. F197–F211, Mar. 2008.
- [12] M. S. Zhdanov, *Geophysical Electromagnetic Theory and Methods*. Amsterdam, The Netherlands: Elsevier, 2009.
- [13] G. W. Hohmann, "Three-dimensional induced polarization and electromagnetic modeling," *Geophysics*, vol. 40, no. 2, pp. 309–324, Apr. 1975.
- [14] H. O. Seigel "Mathematical formulation and type curves for induced polarization" *Geophysics*, vol. 24, pp. 547–565, 1959.
- [15] M. S. Zhdanov, *Geophysical Inverse Theory and Regularization Problems*. Amsterdam, The Netherlands: Elsevier, 2002.
- [16] S. R. Titley, *Advances in Geology of the Porphyry Copper Deposits*. Tucson, AZ, USA: University of Arizona Press, 1982.
- [17] M. Thoman, K. Zonge, and D. Liu, *Geophysical Case History of North Silver Bell, Pima County, Arizona-A Supergene-Enriched Porphyry Copper Deposit*, vol. 42, Spokane, WA, USA Northwest Mining Assoc., 1998.